




RESEARCH ARTICLE | MARCH 26 2019

Photostriction actuation of silicon-germanium bilayer cantilevers **FREE**

V. Chenniappan ; G. A. Umana-Membreno  ; K. K. M. B. D. Silva; M. Martyniuk; A. Keating; J. M. Dell; L. Faraone



Journal of Applied Physics 125, 125106 (2019)

<https://doi.org/10.1063/1.5075525>



View
Online



Export
Citation

CrossMark



AIP Advances

Why Publish With Us?



25 DAYS
average time
to 1st decision



740+ DOWNLOADS
average per article



INCLUSIVE
scope

[Learn More](#)

 AIP
Publishing

Photostriction actuation of silicon-germanium bilayer cantilevers

Cite as: J. Appl. Phys. **125**, 125106 (2019); doi: [10.1063/1.5075525](https://doi.org/10.1063/1.5075525)

Submitted: 23 October 2018 · Accepted: 7 March 2019 ·

Published Online: 26 March 2019



V. Chenniappan,¹ G. A. Umana-Membreno,^{1,a)} K. K. M. B. D. Silva,¹ M. Martyniuk,¹ A. Keating,² J. M. Dell,¹ and L. Faraone¹

AFFILIATIONS

¹School of Electrical, Electronic and Computer Engineering, The University of Western Australia, 35 Stirling Highway, Crawley 6009, Australia

²School of Mechanical and Chemical Engineering, The University of Western Australia, 35 Stirling Highway, Crawley 6009, Australia

^{a)}Author to whom correspondence should be addressed: gilberto.umanamembreno@uwa.edu.au

ABSTRACT

This work presents a study of photostriction-based optical actuation in bilayer cantilevers made of silicon and germanium thin-films and follows previous work in this area on silicon cantilevers. This experimental and theoretical study examines the role of the silicon-germanium heterojunction in optical actuation. It is shown that the germanium layer dominates the mechanical response of the device, which can be exploited to achieve enhanced optical actuation in cantilevers.

Published under license by AIP Publishing. <https://doi.org/10.1063/1.5075525>

I. INTRODUCTION

With the scaling down of micro-electro-mechanical systems (MEMS) to nano-scale dimensions, increased attention is being paid to alternative means of mechanically actuating these devices without the need to make electrical contacts. Optical actuation, which evokes a mechanical response to an optical stimulus, has received considerable research focus,^{1–10} since it is particularly useful in scenarios where electrical contacts are not suitable. Piezoelectric actuation of an AFM cantilever excites not only the desired cantilever mode but also other undesired modes of the AFM probe setup (known as “forest of peaks”). This problem can be completely overcome by optical actuation, which is the technology implemented in Cypher AFMs from Asylum Research.⁴

Optical actuation can be achieved mainly through photothermal effects,^{1–4} radiation pressure,³ photostriction effects,^{5–8} and optical gradient force.^{9,10} Work leading up to the present study analyzed photostriction in silicon microcantilevers fabricated on silicon-on-insulator (SOI) wafers⁷ and established a link between optically excited mechanical response and semiconductor device parameters. Recently, Ramaiah *et al.*⁸ analyzed the contribution of photostrictive and photothermal effects in the deflection characteristics of AFM cantilevers. It is well known that germanium strongly absorbs a broader range of optical wavelengths than silicon and

that the photostriction coefficient of germanium is higher than that of silicon. Hence, it would be of technological interest to study the effect of photostriction in germanium-based MEMS structures. This work examines photostriction in a bilayer cantilever consisting of silicon and germanium thin films.

II. BACKGROUND

The elastic properties of semiconductors are closely related to their electronic properties.¹¹ The volume of a semiconductor crystal is affected by the occupation of electronic energy levels in the conduction and valence bands. Consequently, when electrons are excited across the energy bandgap, semiconductors undergo mechanical strain (dilation or contraction) to minimize the free energy. This strain causes a volume change (ΔV), which is related to the pressure coefficient of the bandgap dE_g/dP by^{12,13}

$$\left(\frac{\Delta V}{V}\right) = \frac{dE_g}{dP} \Delta n, \quad (1)$$

where Δn is the excess carrier density in the semiconductor. The pressure coefficient of the bandgap is positive (5.1×10^{-3} eV/kbar) in germanium and negative in silicon (-1.4×10^{-3} eV/kbar). Hence, when illuminated with photons of energy greater than the

28 July 2023 05:33:35

bandgap energy, silicon undergoes volume contraction and germanium undergoes volume expansion. The excess carrier density Δn is related to the excess carrier lifetime (τ) by

$$\Delta n = G\tau, \quad (2)$$

where G is the carrier generation rate. Hence, with G unchanging, a longer carrier lifetime leads to larger volume change.

Given that germanium undergoes volume expansion when excess carriers are injected, it can be established that the tip of a cantilever made of germanium will undergo downward displacement when its top surface is illuminated with light. Similarly, a silicon cantilever will bend upwards under the same conditions. Previous work has demonstrated the upward deflection of silicon cantilevers when illuminated with a laser light of wavelength 405 nm.⁷

III. SAMPLE PREPARATION

The samples used for the experiments reported here consisted of silicon cantilevers fabricated on silicon on insulator (SOI) substrates. A germanium layer was deposited on a portion of the silicon cantilever using e-beam deposition, to form a bilayer cantilever, with a typical geometry as shown in Fig. 1.

Figure 1(c) shows a top view of the fabricated cantilevers. The silicon cantilevers are of 200 μm length and 20 μm width, and a 50 nm thick layer of germanium was deposited so as to cover different lengths of the silicon cantilevers. In Fig. 1(c), beam 1 has 10% of its length covered with germanium and beam 6 has 90% of its length covered with germanium. This particular variation in germanium layer coverage was chosen to illustrate the effects of photostriction.

IV. EXPERIMENTAL PROCEDURES

The experimental setup consisted of a laser Doppler vibrometer (Polytec Inc.) to measure the deflection of the cantilevers and a 405 nm wavelength laser source for actuation. The vibration sensing laser from the vibrometer and the 405 nm actuation laser were focused onto the cantilever upper surface through the same microscope. The actuation laser had a spot size of 120 μm^2 with a variable intensity that could be varied from a continuous wave to 60 kHz with a 50% duty cycle. A power density of 400 W/cm² was used in all measurements related to this work.

Figure 2(a) shows the fabricated cantilevers along with the vibration sensing laser spots (633 nm wavelength) and the actuation laser spot. The displacement of the cantilever was converted into a voltage signal by a displacement decoder and captured by a digital oscilloscope. The voltage output from the decoder was correlated with the direction of cantilever deflection: a decrease in voltage from zero volts corresponds to the cantilever moving downward and a positive voltage corresponds to an upward deflection.

The following results were obtained with two bilayer cantilevers, 200 μm in length, one with a 20 μm long and a 50 nm thick layer (cantilever 1) of Ge and the other with a 100 μm long layer and a 50 nm thick (cantilever 2) of Ge. In all the experiments, the sensing laser of the vibrometer was placed 10 μm from the tip of the cantilever, and the actuation laser was moved to various

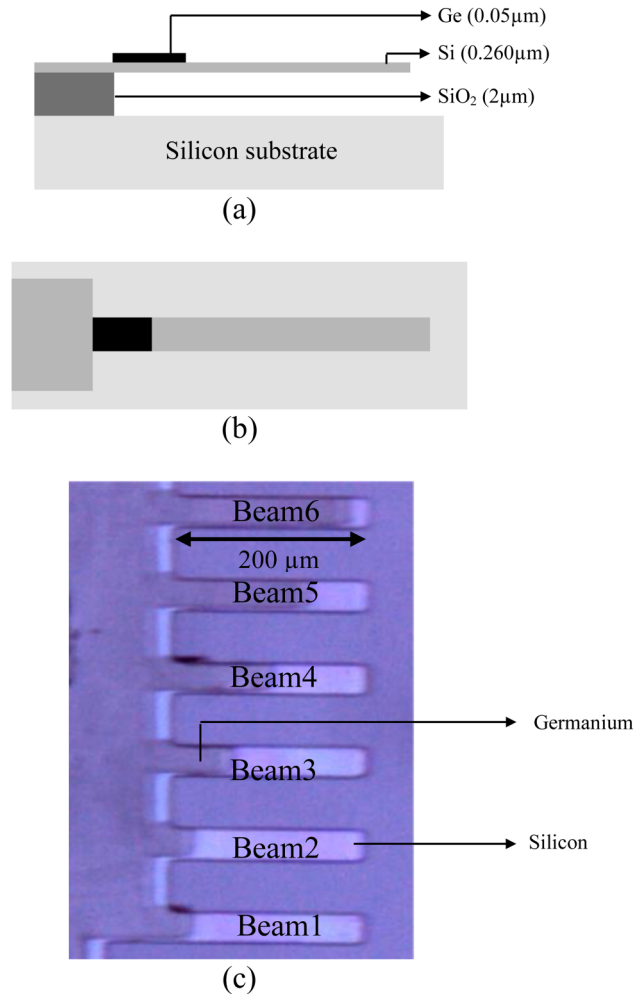


FIG. 1. (a) Schematic illustration of Si-Ge cantilevers (side view), (b) schematic illustration of Si-Ge cantilevers (top view), and (c) image of fabricated cantilevers (top view).

positions along the length of the cantilever. The actuation laser spot was focused at different points along the length of the cantilever (P1, P2 ... P_n) to examine and illustrate the effect of photostriction based deflection of the bilayer cantilevers. Figure 2(b) illustrates the movement of the actuation laser spot along the length of the cantilever. All experiments were carried out at room temperature and pressure.

Photostriction causes silicon to undergo volume contraction and germanium to undergo volume expansion.^{12,13} Based on this fact, it is possible to establish that silicon-only cantilevers would bend upwards (i.e., away from the substrate) when illuminated with light on the top surface of the cantilever, and germanium cantilevers would bend downwards. It is therefore expected that the Si-Ge bilayer cantilevers would deflect upwards when the actuation laser spot is on silicon and downwards when the spot is on germanium.

28 July 2023 05:33:35

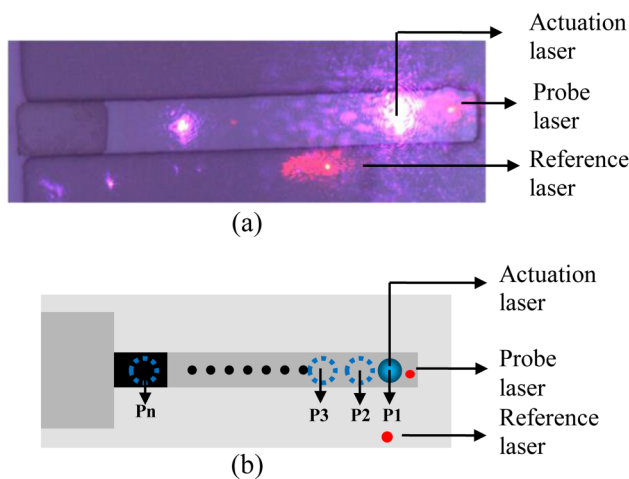


FIG. 2. (a) Laser positions on the cantilevers and (b) an illustration of the movement of the actuation laser spot.

Figure 3(a) shows the beam deflection as a function of time and the actuation laser location on cantilever 1. The actuation laser spot was moved along the length of the cantilever [points P1, P2, etc., as illustrated in Fig. 2(b)]; the deflection of the cantilever was recorded at points spaced apart by $25\ \mu\text{m}$. It is seen that the bilayer cantilever bends upwards when the actuation laser spot is near the tip of the cantilever and bends downwards when the spot is on the germanium layer. The magnitude of upward deflection reduces as the illumination spot on the silicon moves towards the germanium layer. However, the transition from upward deflection to downward deflection occurs when the spot is still on the silicon layer, nearly $40\ \mu\text{m}$ – $50\ \mu\text{m}$ away from the germanium layer. Figure 3(b) shows the result of the same experiment on cantilever 2. Once again, the cantilever bends downwards when the spot is still on the silicon layer, and the cantilever bends downwards even when the spot is at the tip of the cantilever. The magnitude of deflection is almost double that of the cantilever in case 1. A closer look at the nature of deflection in Fig. 3(b) reveals that the cantilever in case 2 starts deflecting upwards initially (laser spot at the tip) and after approximately $0.1\ \text{ms}$, the downward deflection dominates, whereas when the laser spot is closer to the germanium layer, the cantilever bends downwards more rapidly (laser spot at $125\ \mu\text{m}$).

V. DISCUSSION

When cantilevers such as the ones used in this work are excited with laser radiation, they can undergo mechanical deflection due to photothermal effects, photostriction, or radiation pressure. Two characteristics of the cantilever response are used to identify the phenomenon causing the deflection:

1. direction of deflection of the cantilever,
2. temporal behavior of the cantilever deflection—a slower response corresponding to photothermal effects and a faster response corresponding to photostriction.

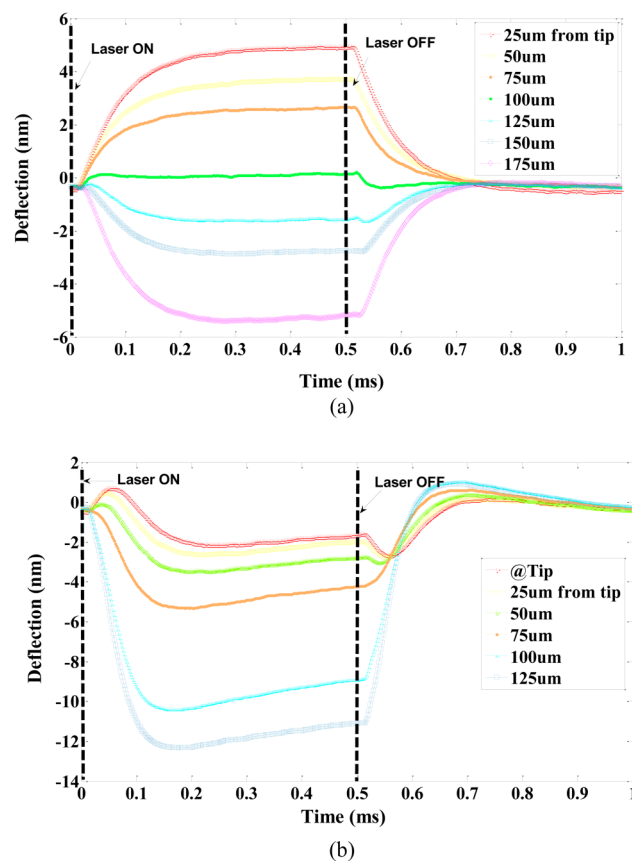


FIG. 3. (a) Deflection of $20\ \mu\text{m}$ -Ge cantilever and (b) deflection of $100\ \mu\text{m}$ -Ge cantilever.

Both silicon and germanium absorb strongly in the UV-blue region (405 nm). The absorbed radiation generates electron-hole pairs and heat. The excess carriers as well as the heat generate mechanical stress leading to the deflection of micro-cantilevers. The stress generation due to excess carriers is known as photostriction, and the stress due to heat is known as photothermal stress. Photothermal stress causes expansion of the material and results in downward displacement of the cantilever. Radiation pressure applies downward force when illuminated from the top of the cantilever and hence causes downward deflection.

In germanium, both photostriction and photothermal effects cause expansion of the material (i.e., tensile stress), whereas in silicon, photostriction results in contraction (compressive stress), and photothermal effects cause expansion (tensile stress). When silicon is illuminated, the excess carriers diffuse throughout the cantilever as well as the anchor region. The silicon layer and the underlying oxide layer form a bilayer. The silicon layer directly in contact with the oxide layer is constrained from undergoing contraction, while the top of the silicon layer is free to undergo contraction, which generates a moment that causes upward deflection of the cantilever. Thus, of the three effects, only photostriction in

28 July 2023 05:33:35

silicon can cause upward deflection of the cantilever (both in the monolayer and Si-Ge bilayer SOI cantilevers). Reference 5 uses both the direction of deflection and time response of the deflection to identify and isolate photostriction and photothermal effects. A detailed analysis of photostriction and photothermal responses requires modeling of spatial and temporal evolution of stress waves.^{1,12–14} For the purpose of this paper, which focuses on the role of a semiconductor heterojunction in the deflection characteristics of the cantilevers, we present a simplified analysis based on static models considering the uniform stress developed due to photostriction and photothermal effects.

The stress generated due to photostriction is given by^{5,7}

$$\frac{1}{3(1-2\nu)} \frac{dE_g}{dP} \Delta n E, \quad (3)$$

where ν is Poisson's ratio and E is Young's modulus of the semiconductor.

In our case where silicon and germanium were used for the experiments, the values are

- (a) Poisson ratio = 0.2 for both Si and Ge,
- (b) $dE_g/dP = 2 \times 10^{-24} \text{ cm}^3$ for Si and $10 \times 10^{-24} \text{ cm}^3$ for Ge,^{12,13}
- (c) $E = 160 \text{ GPa}$ for Si and 103 GPa for Ge.

In the case of silicon, we estimated the value of the photogenerated excess carrier density by a combination of photoconductance decay measurements and simulations. This is reported in detail in our earlier publication.⁷ For a laser power density of 400 W/cm^2 and a laser spot size of $120 \mu\text{m}^2$, we obtained an excess carrier density of $\sim 5 \times 10^{19} \text{ cm}^{-3}$.

Substituting the values in Eq. (3), we obtain a stress of -8.88 MPa for silicon.

We have shown through our analyses that the photogenerated carriers diffuse to the Ge layer from the Si layer. Our measurement results show that the Ge layer dominates the response even when the laser spot is on the Si layer (Fig. 3). Assuming that most of the carriers diffuse to the Ge layer, so that the excess carrier density in the Ge is $\sim 5 \times 10^{19} \text{ cm}^{-3}$, we can calculate the stress generated in Ge, using Eq. (3), as being $+28.3 \text{ MPa}$.

If the laser spot is on the Ge layer, the excess carrier density will be even higher owing to a higher absorption coefficient and a lower bandgap of Ge, and the corresponding stress will also be higher. The above analysis shows that for the case of photostriction, germanium will dominate the deflection characteristics of the cantilever.

The expression for stress developed due to heat is⁵

$$\alpha \Delta T E, \quad (4)$$

where α is the thermal expansion coefficient of the material ($2.6 \mu\text{m/m K}$ for Si and $6.0 \mu\text{m/m K}$ for Ge), ΔT is the rise in temperature due to photo excitation, and E is Young's modulus of the material.

The rise in temperature can be calculated by considering that all the energy incident on the cantilever results in an increase in temperature (this would give an upper limit on the stress generated due to heat). The temperature rise can be evaluated using the

specific heat capacity of the material, i.e.,

$$\text{Energy} = C_p m \Delta T (1 - R), \quad (5)$$

where C_p is the specific heat capacity of the material (0.7 J/g K for Si and 0.32 J/g K for Ge), m (0.63 ng for a Si cantilever of volume $200 \mu\text{m} \times 20 \mu\text{m} \times 0.26 \mu\text{m}$ and 0.16 ng for Ge of volume $20 \mu\text{m} \times 20 \mu\text{m} \times 0.05 \mu\text{m}$) is the mass of the cantilever, and R is the reflectivity of the material (~ 0.5 for Si and Ge at 405 nm).

We used a pulsed laser at 1 kHz with a duty cycle of 50% , so the energy delivered per cycle is 1.2 nJ . Substituting the values in Eq. (5), we get a temperature rise of 1.36 K in Si, which is within the range of typical temperature increases due to photothermal excitation reported in the literature.¹⁴

This value of temperature rises when substituted in Eq. (4) gives a stress of 0.29 MPa , which is less than one-tenth of the stress generated due to photostriction. It should be noted that this is the *maximum* possible stress generated due to photothermal excitation, since we have considered that all the optical power is converted into an increase in temperature. For the case of photostriction, we have obtained the stress value with minimal possible assumptions. In particular, we obtained the excess carrier density based on measurements.

Assuming that all the energy incident is expended to increase the temperature when the laser spot is on the Ge layer, we get a temperature rise of 23.4 K for germanium. This ΔT will generate a stress of 14 MPa , which is much higher than the value obtained for Si. Thus, irrespective of the mechanism causing the deflection, germanium always dominates the response.

To illustrate the effect of stresses developed in the silicon and germanium layers, we carried out simulations in Coventorware software. A cantilever with dimensions given in the above calculations was simulated for three different stress combinations. The results obtained are presented in Fig. 4. For -8.8 MPa stress in Si and 0 MPa stress in Ge, the beam deflects about 600 nm in the upward direction. The deflection is 500 nm for a stress of 5 MPa in germanium and 0 MPa stress in Si. For a combination of -8.8 MPa in Si and 5.3 MPa in Ge, the deflection is about 15 nm in the upward direction.

Analyzing Fig. 3 in the light of the above calculations indicates that in the silicon part of the cantilever, the photostriction effect dominates, since none of the other phenomena cause upward deflection of the cantilever. In germanium, both photothermal and photostrictive effects cause downward deflection of cantilevers, so it is difficult to isolate the contribution of the two effects in germanium. The temporal evolution of deflection in Fig. 3(b) shows a fast upward deflection initially, which is a result of photostriction in silicon, and a slower downward deflection, which ultimately dominates the response. The slower response could be due to the photothermal effect in Ge or it could be due to the delayed photostriction effect in Ge, which is analyzed in Secs. V A and V B. As the germanium layer starts dominating the response of the cantilever even before the laser spot moves on to it, it is evident that the transport of carriers from Si to Ge plays a role in the mechanical response. Thus, a detailed analysis of the transport of carriers based on the band structure of the semiconductors becomes imperative.

28 JULY 2023 05:33:35

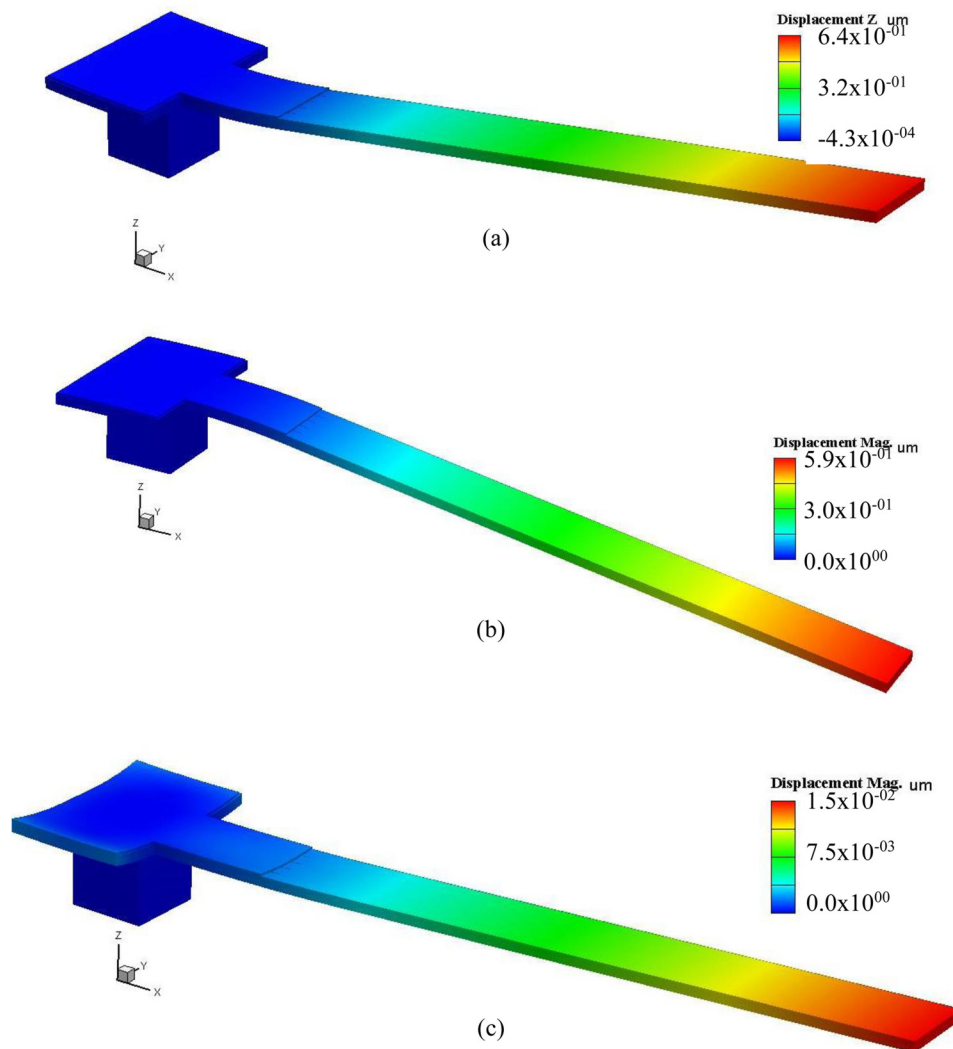


FIG. 4. (a) Cantilever deflection for a stress of -8.8 MPa in Si and 0 MPa in Ge. (b) Cantilever deflection for a stress of 0 MPa in Si and 5 MPa in Ge. (c) Cantilever deflection for a stress of -8.8 MPa in Si and 5.3 MPa in Ge.

28 July 2023 05:33:35

The experimental observations presented in Sec. IV need to be understood in terms of the band structure of silicon and germanium. As the band structure of silicon and germanium is different, a heterojunction is formed when germanium is deposited on silicon. Silicon in the SOI wafer and the e-beam deposited germanium are both p-type, and the germanium layer is amorphous. The doping density of the Si layer is $6 \times 10^{13}/\text{cm}^3$ and of Ge is $5 \times 10^{17}/\text{cm}^3$.¹⁵ Figure 5(a) shows the band structure of silicon and germanium layers used.¹⁶ Simulations were carried out using the Synopsys Sentaurus device simulator to analyze the heterojunction characteristics. Two geometries, one having exactly the same dimensions as the bilayer cantilever and the other having thicker layers of silicon and germanium, were used for simulations. In the latter structure, a $2 \mu\text{m}$ wide silicon-germanium junction with a $3 \mu\text{m}$ thick silicon layer and a $0.5 \mu\text{m}$ thick germanium layer were used purely for ease of discussion. Figures 5(b) and 5(c) show the band diagram and distribution of space charge in the

heterojunction, respectively. Discontinuities exist in both the valence band and the conduction band. When the junction is formed, holes, the majority carriers on both sides, find lower energy states available on the germanium side and flow from silicon to germanium. This flow forms a depletion layer in the lightly-doped silicon, and the holes accumulate at the heterojunction. The band diagram in Fig. 5(b) shows that the depletion region is present only on the silicon side of the junction.

Analytical calculations were also carried out to corroborate the simulation results. Based on the doping data, a depletion layer width in the silicon of approximately $2.0 \mu\text{m}$ and a built-in potential of 0.23 V were calculated. However, since the silicon layer in the experimental samples is thin (260 nm), it will be fully depleted under Ge and will extend along the length of the cantilever [Fig. 6(a)]. Device simulations show that the silicon layer directly underneath the Ge layer is depleted and the depletion region extends up to one micron along the length of the silicon layer

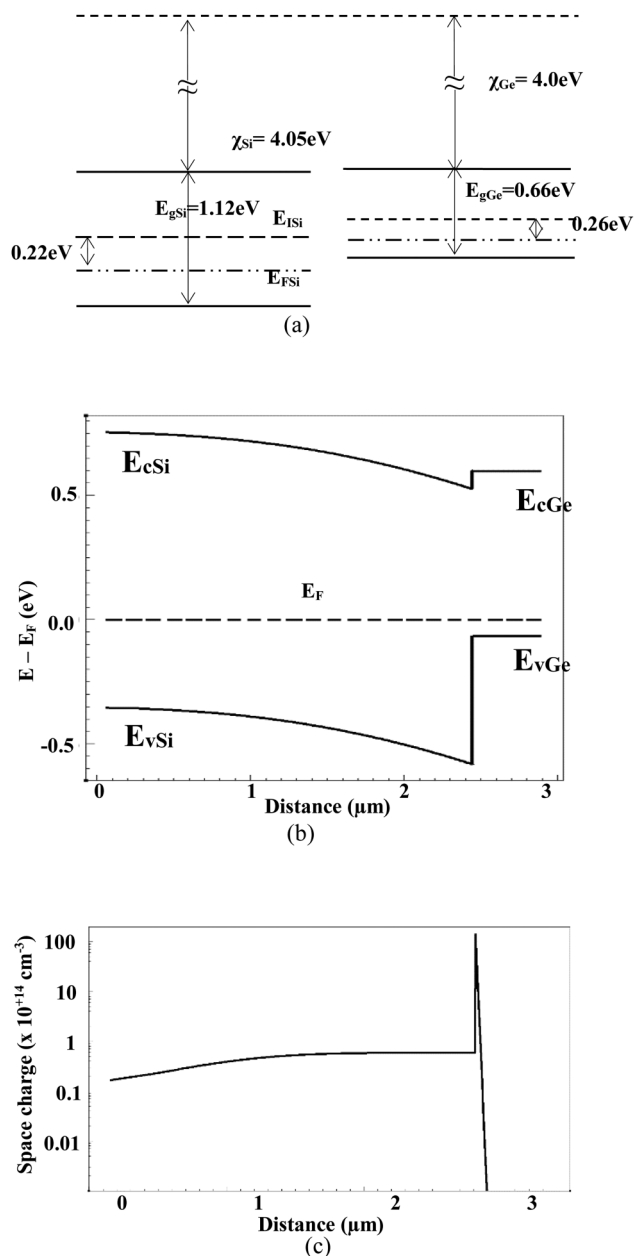


FIG. 5. (a) Band structure of Si and Ge, (b) band structure of the heterojunction, and (c) corresponding space charge near the heterojunction.

[Fig. 6(b)]. Figure 6(c) shows the calculated hole density along the length of the silicon layer. The turn-on voltage of the junction measured with a semiconductor parameter analyzer and a probe station is found to be 0.3 V , as shown in the current-voltage (I-V) characteristics presented in Fig. 7.

The lifetime of carriers in the SOI silicon was estimated to be $27 \mu\text{s}$ using photoconductive decay measurements.⁷ The 405 nm

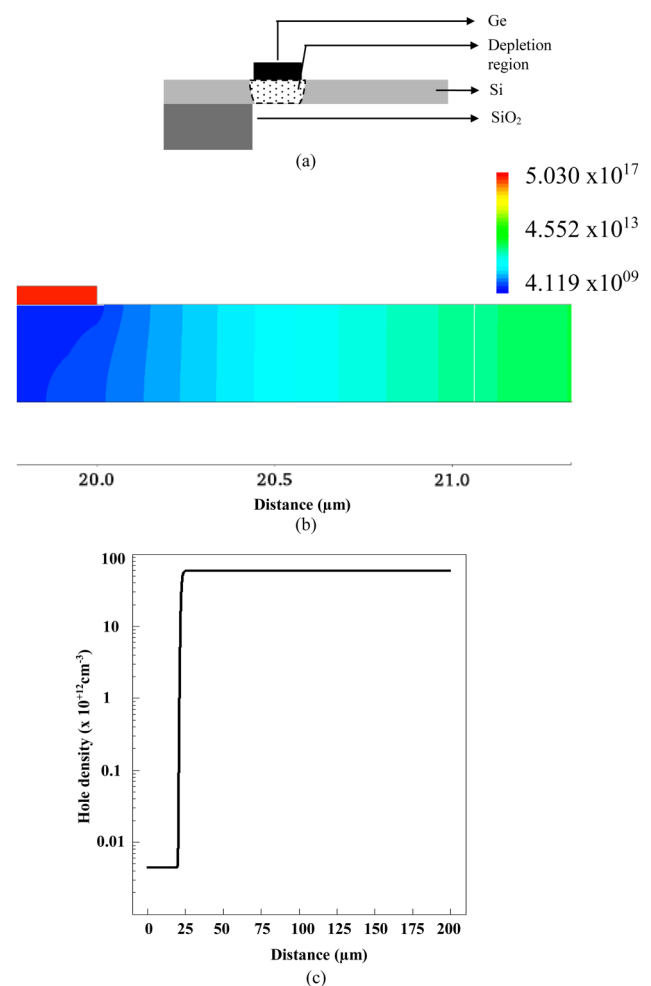


FIG. 6. (a) Illustration of the silicon depletion layer, (b) expanded view of the hole density near the edge of the heterojunction, and (c) hole density along the length of the silicon layer.

laser, which was used for the optical actuation experiments, was also used for these measurements. The lifetime of $27 \mu\text{s}$ corresponds to a diffusion length of $180 \mu\text{m}$, which is almost the full length of the cantilevers used for optical actuation. For the laser power density used in the experiments (400 W/cm^2), the device will be operating in the high-injection regime, i.e., the photogenerated excess carrier density will be higher than the doping density, and hence, photogenerated carriers dominate the device behavior.

A. Case 1 (cantilever with a $20 \mu\text{m}$ long Ge layer)

When the cantilever was optically excited with the actuation laser at the tip, the generated electron-hole pairs diffuse to the depletion region, which results in a reduction in depletion layer width. The excess carriers recombine, and some fraction reach the germanium layer. The amount of volume contraction caused by

28 July 2023 05:33:35

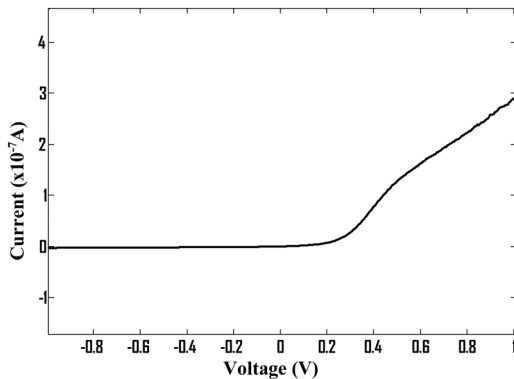


FIG. 7. I-V characteristics of the Si-Ge heterojunction.

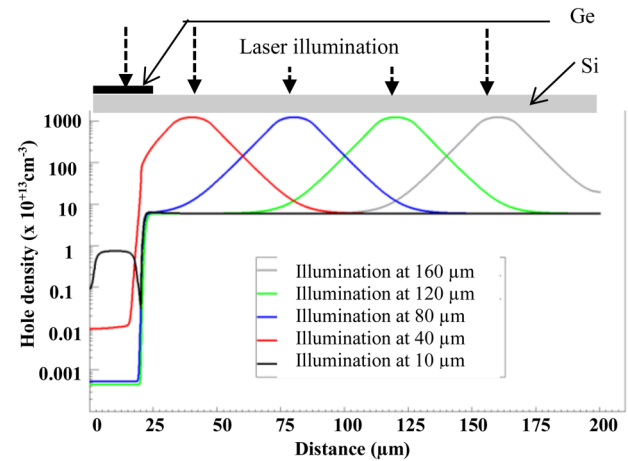
excess carriers in the silicon dominates in comparison to the amount of volume expansion caused by the excess carriers reaching the germanium layer. As a result, the mechanical response of the cantilever is dominated by the silicon layer [Fig. 3(a)] as is evident from the upward deflection of the cantilever for laser excitation beyond $100\text{ }\mu\text{m}$ from the Ge layer edge. However, as the actuation laser spot is moved closer to the depletion layer edge, the number of excess carriers reaching the germanium layer increases relative to the number in the silicon, and eventually, the Ge volume expansion dominates, resulting in downward deflection of the cantilever [Fig. 3(a)] for laser excitation within $100\text{ }\mu\text{m}$ of the Ge layer edge. Since the stress generation due to heat in silicon is very low, the response of the cantilever is dominated by photostriction as long as the spot is on the silicon layer.

B. Case 2 (cantilever with a $100\text{ }\mu\text{m}$ long Ge layer)

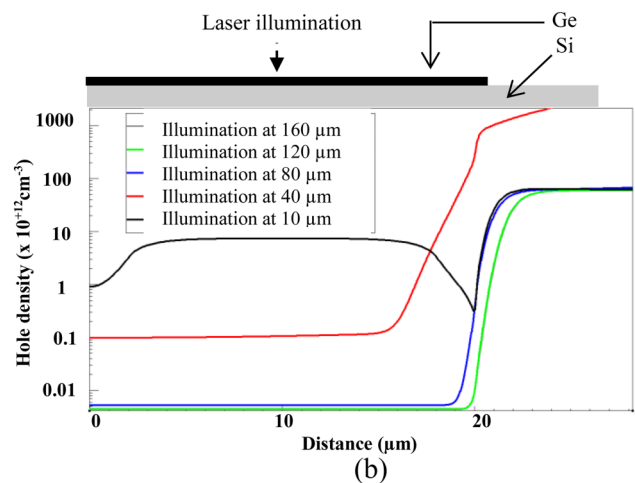
In this case, the number of carriers reaching the germanium layer is higher than in Case 1 for all positions of the excitation laser. As a result, the germanium layer completely dominates the mechanical response. The initial upward deflection of the cantilever (for approximately 0.1 ms) seen in Fig. 3(b) is likely due to the junction capacitance and resistance, which form an RC delay for carriers reaching the germanium layer, resulting in the carriers generated in the silicon causing an initial upward deflection.

In addition to photostriction, the photothermal effect also could play a role in downward deflection of the cantilever. The carriers generated in the Si may thermalize resulting in a temperature rise, and since the rise in temperature in Ge is higher as noted in the previous calculations, a strong bilayer effect is generated resulting in downward deflection of the cantilever. Thus, the slower downward deflection could be due to the RC delay of the heterojunction and/or due to photothermal effects, which is an inherently slower phenomenon than photostriction.

In all cases, the mechanical behavior is dominated by the diffusion of photogenerated excess carriers. The photogeneration of carriers in the heterojunction cantilever was simulated using the Sentaurus device simulator to correlate with the observed mechanical response of the cantilevers. A heterojunction with a $20\text{ }\mu\text{m}$ long



(a)



(b)

FIG. 8. (a) Hole density along the length of the Si layer for laser illumination at various positions and (b) the corresponding hole density in silicon directly under the germanium layer.

germanium layer on top of a $200\text{ }\mu\text{m}$ silicon layer was illuminated at different points along the length of the device with 405 nm light at a power of 10 W/cm^2 . Figure 8 shows the calculated hole density along the length of the silicon layer. When the illumination spot is on the silicon layer, i.e., when the spot is at $160\text{ }\mu\text{m}$, $120\text{ }\mu\text{m}$, $80\text{ }\mu\text{m}$, and $40\text{ }\mu\text{m}$, the hole density is highest at the point of illumination and decreases to a lower value in the region under the germanium layer. As expected, the hole density under the Ge layer increases as the spot moves closer to the Ge/Si boundary. When the spot is at $40\text{ }\mu\text{m}$, the hole density in the silicon layer under germanium is $\sim 1 \times 10^{11}/\text{cm}^3$ and decreases to $5 \times 10^9/\text{cm}^3$ when the spot is at $80\text{ }\mu\text{m}$. Beyond $80\text{ }\mu\text{m}$, there is very little difference in the hole density in the underlying silicon layer, as is evident from Fig. 8(b). When the spot is on the germanium layer, i.e., at $10\text{ }\mu\text{m}$,

28 July 2023 05:33:35

a fraction of the photogenerated carriers reach the silicon layer, forward biasing the junction.

In conclusion, it has been found that the germanium layer dominates the mechanical response of the heterojunction cantilever for the following reasons:

1. The photostrictive coefficient of germanium is larger in magnitude in comparison to that of silicon.
2. In silicon, the photostrictive response causes volume contraction, which deflects the cantilever upwards, whereas a photo-thermal response would cause volume expansion and a downward deflection. In germanium, both effects cause volume expansion, so the combined effect is greater.

VI. SUMMARY

This paper has analyzed the effect of a silicon-germanium heterojunction on the photostrictive response of bilayer cantilevers. The use of an overlying germanium layer enhances the mechanical deflection of the cantilevers, since germanium has a higher pressure coefficient of the bandgap. In addition to enhancing the magnitude of deflection, by suitably patterning the germanium layer on the silicon cantilevers, a particular mode of deflection can be enhanced while suppressing other modes. As photostriction causes a change in the interatomic distance in semiconductors, the material properties such as Young's modulus will be affected,¹¹ thus causing a change in the resonance frequency of the beams.^{17,18} The extent of these variation needs further study.

ACKNOWLEDGMENTS

The authors would like to thank the Australian Research Council (ARC), Australia India Strategic Research Fund (AISRF), and the WA-node of the Australian National Fabrication Facility (ANFF) for support of this work. The authors thank Dr. N. D. Akhavan for assistance in performing device simulations and Dr. B. Cheah and Dr. H. Kala for their assistance in device

fabrication and the experiments. The first author also wishes to thank Dr. K. Majumdar (Department of Electrical Communication Engineering, Indian Institute of Science) for useful discussions.

REFERENCES

- ¹D. Ramos, J. Tamayo, J. Mertens, and M. Calleja, *J. Appl. Phys.* **99**, 124904 (2006).
- ²L. H. Han and S. Chen, *Sens. Actuators A* **121**, 35 (2005).
- ³M. Vassalli, V. Pini, and B. Tiribilli, *Appl. Phys. Lett.* **97**, 143105 (2010).
- ⁴A. Labuda, J. Cleveland, N. A. Geisse, M. Kokun, B. Ohler, R. Proksch, M. B. Viani, and D. Walters, *Micros. Microanal. SPM Suppl.* **21**(March/April), 21–25 (2014).
- ⁵P. G. Datskos, S. Rajic, and I. Datskou, *Appl. Phys. Lett.* **73**(16), 2319 (1998).
- ⁶D. M. Todorovic, B. Cretin, Y. Q. Song, and P. Vairac, *J. Appl. Phys.* **107**, 023516 (2010).
- ⁷V. Chenniappan, G. A. Umana-Membreno, K. K. M. B. D. Silva, H. Kala, A. Keating, M. Martyniuk, J. M. Dell, and L. Faraone, *IEEE J. Microelectromech. Syst.* **24**(1), 182 (2015).
- ⁸M. R. Ramaiah, K. Prabhakar, and S. Tripura Sundari, *Ultramicroscopy* **194**, 215 (2018).
- ⁹M. Li, W. H. P. Pernice, C. Xiong, T. Baher-Jones, M. Hochberg, and H. X. Tang, *Nature* **456**, 480 (2008).
- ¹⁰D. Van Thourhout and J. Roels, *Nat. Rev.* **4**, 211 (2010).
- ¹¹R. W. Keyes, *IBM J.* **5**(4), 266 (1961).
- ¹²T. Figielski, *Phys. Status Solidi* **1**, 306 (1961).
- ¹³W. B. Gauster, *Phys. Rev.* **187**(3), 1035 (1969).
- ¹⁴V. Pini, B. Tiribilli, C. M. C. Gambi, and M. Vassalli, *Phys. Rev. B* **81**, 054302 (2010).
- ¹⁵W.-J. Lee, "Investigation of thin film CdTe/Ge tandem solar cells," Ph.D. thesis (School of Electrical, Electronic and Computer Engineering, The University of Western Australia, 2017).
- ¹⁶D. Woods, *Optoelectronic Semiconductor Devices* (Prentice-Hall, New York, 1994).
- ¹⁷V. Pini, J. J. Ruz, P. M. Kosaka, O. Malvar, M. Calleja, and J. Tamayo, *Sci. Rep.* **6**, 29627 (2016).
- ¹⁸J. J. Ruz, V. Pini, O. Malvar, P. M. Kosaka, M. Calleja, and J. Tamayo, *AIP Adv.* **8**, 105213 (2018).

28 JULY 2023 05:33:35